ELSEVIER

S0032-3861(96)00880-4

Polymer Vol. 38 No. 13, pp. 3333–3346, 1997

0032-3861/97/$17.00 + 0.00

Structures and properties of the water-soluble self-acid-doped conducting polymer blends: sulfonic acid ring-substituted polyaniline/poly(vinyl alcohol) and poly(aniline-*co*-*N*-propanesulfonic acid aniline)/poly(vinyl alcohol)

Show-An Chen* and Gue-Wuu Hwang
Department of Chemical Engineering, National Tsing-Hua University, Hsinchu, Taiwan 30043, China
(Received 12 September 1996)

Blends of the water-soluble self-acid-doped conducting polyanilines, sulfonic acid ring-substituted polyaniline (SPAN) and poly(aniline-*co*-*N*-propanesulfonic acid aniline) (PAPSAH), each with poly(vinyl alcohol) (PVA) were prepared and characterized by X-ray diffraction, X-ray photoelectron spectroscopy, electronic spectroscopy, infra-red spectroscopy, thermogravimentric analysis, conductivity measurements, atomic force microscopy, and scanning tunnelling microscopy. It was found that the incorporation of PVA has no effect on the doping levels of SPAN and PAPSAH in the blends. This is due to the higher basicity of the –N= than –OH, causing a more favourable interaction of the $-SO_3H$ group with –N=. The strong interaction of these polyanilines with PVA through hydrogen bonding between hydroxyl groups (of PVA) and amine and positively charged amine and imine sites (of SPAN and PAPSAH) leads to a decrease in hydrogen bonding among PVA subchains and to a partial miscibility. As the PVA content is higher than 70%, interconnected regions of PVA-rich phase and of SPAN-rich phase are formed such that the dilution effect of PVA on the conductivity is not large. Although SPAN has a much higher thermal undoping temperature (190°C) than PAPSAH (110°C), it reduces to 110°C in the blends due to the occurrence of dehydration at this temperature, while for the blend of PAPSAH with PVA, its thermal undoping temperature remains unchanged. © 1997 Elsevier Science Ltd.

(Keywords: polyaniline; self-acid-doped polymer; water-soluble polymer)

INTRODUCTION

Polyaniline (PAn) is the conjugated conducting polymer that can be doped either by protonation with a protonic acid or charge-transfer with an oxidation agent[1–4]. Its electronic and optical properties can be controlled reversibly by varying the doping level[2]. PAn can be used as an electrode material for organic batteries[5,6], in microelectronics[7–9], as electrochemical chromic material for displays[10,11], and as antistatic coating and electromagnetic shielding material[12,13] Owing to its good environmental stability in doped and neutral states[14,15], PAn is currently considered to have high potentiality toward practical applications.

In many cases, for polyanilines, being soluble and processable is sometimes more important than being highly conductive. In the past few years, much progress has been made to improve both aspects through: polymerization of ring- or *N*-substituted aniline derivatives[16–23]; copolymerization of aniline with a suitable substituted aniline[24–29]; post-treatment of polyaniline with sulfonation on the aromatic rings[30,31], with an incorporation of alkylsulfonic acid[32–34] or alkyl[35] pendant groups on the nitrogen atoms, and with use of functional dopants[36]; control of molecular weight[37]; microemulsion polymerization of aniline[38]; and polymerization of aniline monomers on a template such as a polymeric acid[39–42].

Among these areas of progress, the approach of post-treatment of emeraldine base form of PAn by the sulfonation and incorporation of alkylsulfonic acid pendant groups on the nitrogen atoms is more attractive, as this eliminates the use of external dopants whose stabilities have always been a problem associated with many practical applications of the material. Very recently, the aqueous solutions of self-acid-doped polyanilines were successfully prepared by us[33,34,43] and their free-standing films can be obtained by casting directly from their aqueous solutions, giving conductivities of 1×10^{-2} and 3×10^{-2} S cm^{-1} for sulfonic acid ring-substituted polyaniline (SPAN) and poly(aniline-*co*-*N*-propanesulfonic acid aniline) (PAPSAH), respectively. However, the films are brittle, which limits them from practical applications. One approach for improving their

* To whom correspondence should be addressed

mechanical properties is to blend them with conventional polymers that possess good mechanical properties. In this work, the self-acid-doped polyanilines, SPAN and PAPSAH, were blended with the water soluble polymer, poly(vinyl alcohol) (PVA), in water for improving their processability and flexibility. Compatibilities and relationships between structures and properties of the blends are explored.

EXPERIMENTAL

Syntheses of polymers and preparation of polyblends

The emeraldine base form of PAn was synthesized by use of the chemical oxidation method similar to that of Chiang and MacDiarmid[2]. It was then converted to SPAN by sulfonation of the emeraldine base as described by Yue and coworkers[30,31], and to PAPSAH by reaction with NaH and then propanesultone as reported in our previous works[33,34]. In order to prepare the aqueous solutions of SPAN and PAPSAH, a two-step procedure[33,34,43] for post treatment was performed. SPAN (or PAPSAH) was first dissolved in a NaOH aqueous solution and then purified to remove excess NaOH by dialysis with a semi-permeable membrane in deionized water. The SPANNa (or PAPSANa) aqueous solution so obtained was then converted to SPAN (or PAPSAH) by exchanging Na^+ for H^+ using H^+-type ion-exchange resin to give a stable SPAN (or PAPSAH) aqueous solution.

The blends of SPAN/PVA and PAPSAH/PVA with various compositions were prepared by mixing various amounts of PVA with SPAN and PAPSAH in water, respectively, according to the following procedure. First PVA was fully dissolved in water at 80°C and then cooled to room temperature. Next, various amounts of the PVA aqueous solution were added to each of the SPAN and PAPSAH aqueous solutions, and stirred until each solution was homogeneous. The solutions were coated on glass plates or cast in Teflon moulds to give thin films, which were then subjected to dynamic vacuum at 90°C for removing residual water. For convenience, the SPAN/PVA blends, which contain 10, 30, 50, 70, and 90 wt% of PVA, are designated as S9V1, S7V3, S5V5, S3V7, and S1V9, respectively; the PAPSAH/PVA blends, which contain 40, 50, 70 and 90 wt% of PVA, are designated as P6V4, P5V5, P3V7, and P9V1, respectively.

For preparations of PVA films, the fully dissolved PVA aqueous solution was cooled from 80°C to room temperature, and then cast into films using the same procedures as for the blends.

Characterizations

X-ray photoelectron spectroscopy (X.p.s.), infra-red spectrophotometry (i.r.), u.v.–vis–n.i.r. spectrophotometry, thermogravimetric analysis (t.g.a.), and conductivity measurement, as well as sample preparations and measurement conditions, were described in detail in our previous works[34,43].

X-ray diffraction (X.r.d.) were measured using a Rigaku Model D/Max-2B diffractometer at room temperature. The X-ray beam was nickel-filtered Cu–K_α ($\lambda = 1.54$ Å) radiation from a sealed tube operated at 30 kV and 20 mA. Diffraction intensity data from 5 to 35° (2θ) were obtained at a scan rate of $1° \text{ min}^{-1}$.

Atomic force microscopy (AFM) and scanning tunnelling microscopy (STM) scans were both performed using a Nanoscope III instrument from Digital Instruments. For the AFM technique, a very sharp probe on a flexible cantilever contacted the sample surface to sense the topography of the sample, and an optical head was used to sense the cantilever deflection by sensing the change in position of a laser beam which was reflected off the back of the cantilever. The scan speeds were kept to less than 4.1 Hz per line for a 512 × 512 data array. The STM experiments were performed in air using mechanically prepared Pt/Ir (80/20 by weight) tips. The STM was run in a constant-current mode with a bias voltage of 500 mV and a tunnelling current of 200 pA, at a scan speed of less than 4.1 Hz per line for a 512 × 512 data array. The polymer aqueous solutions were coated on a highly ordered pyrolytic graphite (HOPG) substrate, and then dried by evaporation of water at room temperature, followed by a further drying under dynamic vacuum. The so-obtained films on HOPG surface were scanned by STM and then AFM immediately in air. All images obtained for this paper are real-time photographs taken directly from the computer screen.

RESULTS AND DISCUSSION

Electrical conductivities, molecular interactions and morphological structures of SPAN/PVA and PAPSAH/PVA blends

The results of conductivity measurement on the SPAN/PVA and PAPSAH/PVA blends at room temperature are listed in *Tables 1* and *2*, respectively. The conductivities of the SPAN and PAPSAH at room temperature are about 10^{-2} S cm^{-1}. When blended with 30–40 wt% PVA, their conductivities drop only slightly by one order. As PVA content increases to 50–70 wt% and 90 wt%, they drop by two and three orders, respectively. These results indicate that the incorporation of PVA into the two self-acid-doped PAns provides an insignificant dilution effect on conductivity. They also reflect that an undoping due to the presence of PVA does not occur, and that the PAns must form a continuous network in the blends at the high PVA content (70–90 wt%). Detailed descriptions on these two inferences are given below.

X.r.d. patterns of the PVA film, SPAN/PVA blend films, and SPAN powder are shown in *Figure 1*; and those of PAPSAH/PVA blend films and PAPSAH powder in *Figure 2*. For SPAN powder, the X.r.d.

Table 1 Conductivities at room temperature and maximum conductivities of SPAN and SPAN/PVA blends from conductivity measurements[a] at various temperatures.

Sample	Composition SPAN/PVA (wt ratio)	σ_{RT} (S cm^{-1})[b]	T_{max} (°C)[c]	σ_{max} (S cm^{-1})[d]
SPAN	10/0	1×10^{-2}	190	9×10^{-2}
S7V3	7/3	4×10^{-3}	–	–
S5V5	5/5	6×10^{-4}	115	2×10^{-3}
S3V7	3/7	2×10^{-4}	110	1×10^{-3}
S1V9	1/9	5×10^{-5}	–	–

[a] Using the four-probe method
[b] The conductivity at room temperature before heating scan
[c] The temperature at which the conductivity reach a maximum
[d] The maximum conductivity

Table 2 Conductivities at room temperature and maximum conductivities of PAPSAH and PAPSAH/PVA blends from conductivity measurements[a] at various temperatures.

Sample	Composition PAPSAH/PVA (wt ratio)	σ_{RT} (S cm^{-1})[b]	T_{max} (°C)[c]	σ_{max} (S cm^{-1})[d]
PAPSAH	10/0	3×10^{-2}	110	9×10^{-2}
P6V4	6/4	1×10^{-3}	–	–
P5V5	5/5	9×10^{-4}	100	4×10^{-3}
P3V7	3/7	3×10^{-4}	110	1×10^{-3}
P1V9	1/9	8×10^{-5}	–	–

[a] Using the four-probe method
[b] The conductivity at room temperature before heating scan
[c] The temperature at which the conductivity reach a maximum
[d] The maximum conductivity

pattern exhibits a broad amorphous diffraction peak at about 21°. For PVA, a sharp diffraction peak at $2\theta = 19.5°$ is observed, reflecting a high degree of crystallinity, which is due to the occurrence of strong inter- and intra-molecular hydrogen bonding[44]. After blending of PVA with SPAN, no new crystalline form is generated and the PVA crystalline characteristic still retains. However, as 10% by weight of PVA is incorporated (S1V9, curve b) the peak intensity at 19.5° decreases remarkably to such an extent that the crystalline portion of PVA in the blend (the area above the dash line) is only about one third that of the pure PVA, much lower than the content of PVA, 90 wt%. Although the blends are of two-phase structure, strong interactions between the two components must occur. For the PAPSAH/PVA blends, similar results are also observed.

X.p.s. N(1s) spectrum of the blend of SPAN with PVA, S5V5 film is shown in *Figure 3a*. As for that of SPAN[43], it can be deconvoluted into three component peaks, centered at 401.8 ± 0.1 eV with a FWHM of 1.9 eV, at 400.2 ± 0.1 eV with a FWHM of 1.9 eV, and at 399.3 ± 0.1 eV with a FWHM of 1.6 eV. The area fractions of these three peaks are 0.23, 0.29, and 0.48, respectively. The peak centered at 400.2 ± 0.1 eV is attributed to the radical cation nitrogen[34], which is 29% of the total nitrogen atoms, implying that the SPAN in S5V5 blend has nearly the same fraction of radical cation nitrogen (or same doping level) as in the SPAN (30%)[43]. For the blend of PAPSAH with PVA, P5V5 film, its X.p.s. N(1s) spectrum is shown in *Figure 3b*. After a deconvolution, the spectrum gives three component peaks at 401.8 ± 0.1 eV with a FWHM of 2.0 eV (iminium ions, 17% of the total area), 400.2 ± 0.1 eV with a FWHM of 1.5 eV (radical cation nitrogen, 33%), and 399.3 ± 0.1 eV with a FWHM of 1.5 eV (uncharged amine nitrogen, 50%), implying that P5V5 has a doping level of 0.33, the same as that of PAPSAH[34]. These results indicate that the incorporation of PVA into the SPAN and PAPSAH has no effect on their doping levels. The reason is that the basicity of the –N= unit is higher than that of the –OH= group, which leads to a more favourable interaction of the acid group, $-SO_3H$, with the –N= unit.

U.v.–vis spectra of SPAN and the blend S5V5 are shown in *Figure 4a*. Both systems have the same absorption peaks at 313 nm (π–π^* transition[45]), 380–420 nm (polaron band[46]), and 580 nm (exciton transition of the quinoid rings[47]). While the absorption peak at

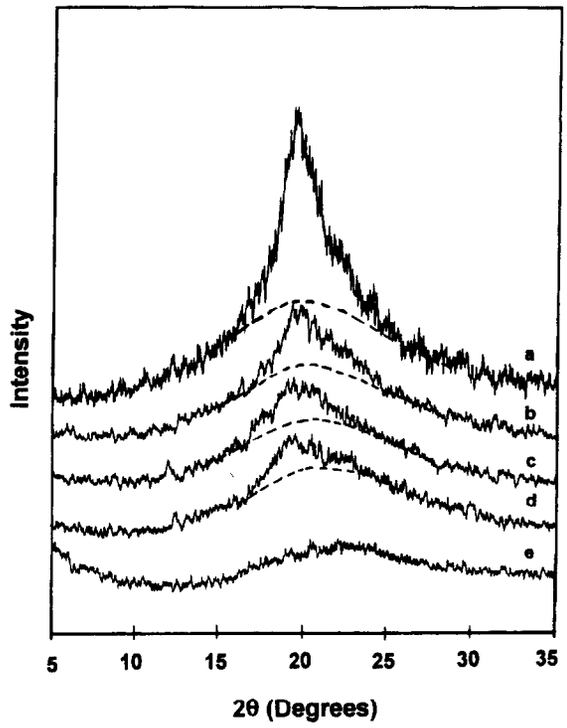

Figure 1 X.r.d. patterns of (a) PVA, (b) S1V9, (c) S3V7, (d) S5V5, and (e) SPAN

880 nm (polaron band[46]) for SPAN is broader than that for S5V5. These results would indicate that although the doping level has not been changed after the blending as determined by X.p.s. above, the polarons in the SPAN of the blends are more localized than those in the pure SPAN. Similar results for PAPSAH and its blend with PVA, P5V5, are also observed (see *Figure 4b*).

I.r. spectra of PVA, SPAN and S5V5 are shown in *Figure 5* (curves *a*, *b* and *c*). The absorption band at 1577 cm^{-1} of SPAN (C=C ring stretching of IP$^{\cdot+}$, where IP$^{\cdot+}$ is the radical cation of imino-1,4-phenylene)[48,49] shifts by 7 cm^{-1} to 1584 cm^{-1} after the blending, which is due to the decrease of polaron delocalization as described in the u.v.–vis section. The band at 1143 cm^{-1} of PVA, assigned to C–O stretching[50], shifts by 4 cm^{-1} to 1147 cm^{-1} and the $C_{aromatic}$–N stretching at 1301 cm^{-1} of SPAN shifts by 2 cm^{-1} to 1303 cm^{-1}, which are due to the formation of hydrogen bonding between hydroxyl groups of (PVA) and amine and positively

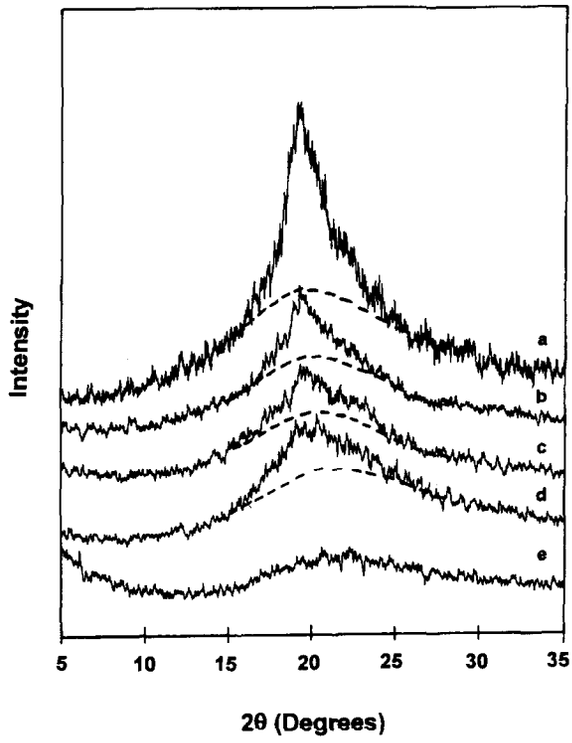

Figure 2 X-ray diffraction patterns of (a) PVA, (b) P1V9, (c) P3V7, (d) P5V5, and (c) PAPSAH

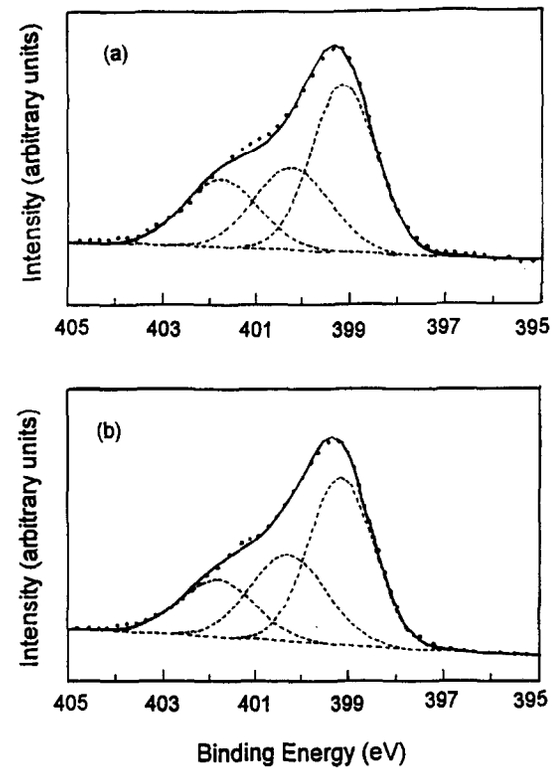

Figure 3 N(1s) X.p.s. core-level spectra of (a) S5V5 and (b) P5V5

charged amine and imine sites (of SPAN) as shown below:

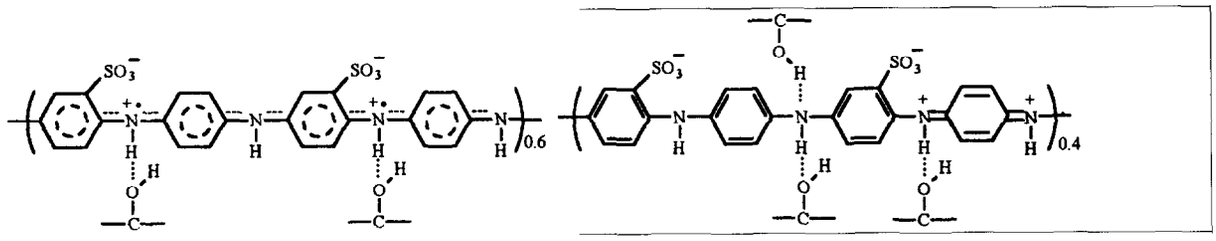

The formation of hydrogen bonding between the two components would cause a decrease in crystallinity of PVA in the blends as was already confirmed in the results of X.r.d. above. For the blend of PAPSAH with PVA, P5V5, similar results as for the blend of SPAN with PVA are found. The absorption band of the C=C ring stretching of $IP^{\cdot+}$ shifts from 1572 cm^{-1} by 9 cm^{-1} to 1581 cm^{-1} after the blending due to the decrease of polaron delocalization. The C–O stretching shifts from 1143 cm^{-1} by 12 cm^{-1} to 1155 cm^{-1} and the $C_{aromatic}$–N stretching at 1315 cm^{-1} increases by 3 cm^{-1} as compared to that of PAPSAH at 1312 cm^{-1} (*Figure 5e*) due to the formation of hydrogen bonding between the hydroxyl groups (of PVA) and amine and positively charged amine and imine sites (of PAPSAH), as shown below:

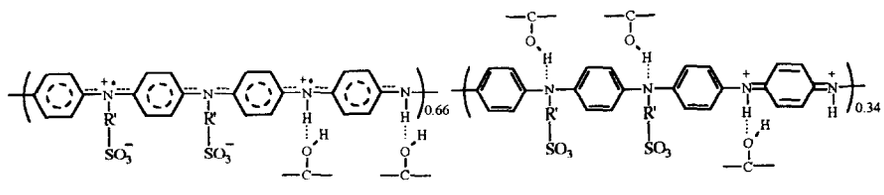

(where R' = —$(CH_2)_3$—)

AFM and STM were used to investigate the morphological structure of SPAN/PVA blends. *Figures 6a–6f* show the AFM images of the SPAN and SPAN/PVA blends films coated on HOPG substrates from their aqueous solutions. As can be seen, the surface morphology of SPAN is different from those of SPAN/PVA blends. The SPAN exhibits an aggregated granules morphology, while the films of the SPAN/PVA blends all have a much smoother surface morphology, in which no significant difference in morphology due to composition variation can be observed. *Figures 7a–7f* show the STM images of the above samples. The STM image of SPAN (*Figure 7a*) is similar to, but sharper in contrast than, its AFM image (*Figure 6a*). The STM images of S9V1 (10 wt% PVA) and S7V3 (30 wt% PVA) (*Figures 7b* and *7c*) are similar to their corresponding AFM images (*Figures 6b* and *6c*). As the PVA content increases

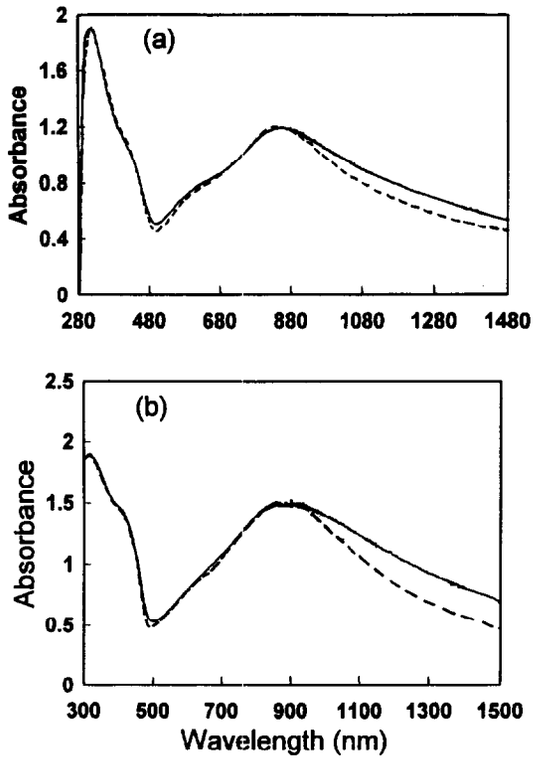

Figure 4 U.v.–vis spectra of (a) SPAN, ———, and S5V5, - - - - -, solid films; (b) PAPSAH, ———, and P5V5, - - - - -, solid films

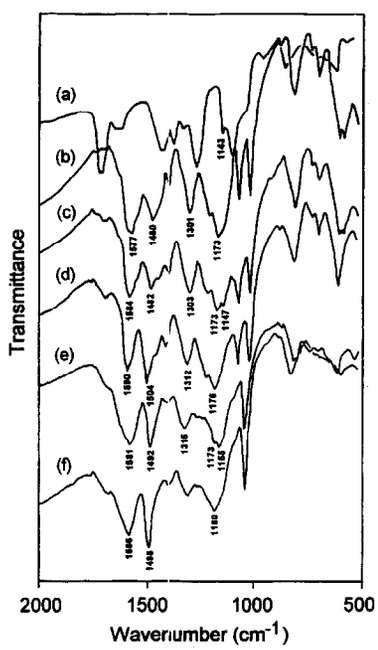

Figure 5 I.r. spectra of (a) PVA, (b) SPAN, (c) S5V5, (d) S5V5 after thermal treatment by heating at 150°C for 1 h under dynamic vacuum; (e) P5V5, and (f) P5V5 after thermal treatment by heating at 150°C for 1 h under dynamic vacuum

to 50 wt% (S5V5) (*Figure 7d*), the contrast of the bright and dark regions becomes sharper; the bright region is referred to as the SPAN-rich phase (having a higher conductivity) and the dark region as the PVA-rich phase (having a lower conductivity). Both the dark region and the bright region (size about 5 μm) are composed of several granular aggregates of size about 0.5–1 μm, and the white regions start to form a continuous network. The extent of phase separation becomes more obvious in the blends with PVA higher than 70 wt% (S3V7 and S1V9) (*Figures 7e* and *7f*). Even though the PVA is the major component in S3V7 and S1V9, the SPAN or SPAN-rich phase (the bright region) still forms a continuous network. A similar result has been observed by Yang *et al.*[51] in the blend of camphor sulfonic acid doped PAn (CSA–PAn) with poly(methyl methacrylate) (PMMA), even though the blend contains only 2 wt% CSA–PAn. This is probably the reason why the PVA dilution effect on conductivity is insignificant as such the conductivity only drops by a factor of 10^2 to 10^3 as the PVA content is 90 wt% (*Table 1*). These results indicate that PVA and SPAN in the blends of SPAN/PVA are partially miscible, and binodal type phase separation exists in the blends with PVA lower than 50 wt% and spinodal decomposition occurs with PVA higher than 70 wt%. As PVA content is minor (lower than 50 wt%) it disperses in SPAN matrix fairly well. As PVA is the major component (higher than 50 wt%), interconnected regions of PVA-rich phase and of SPAN-rich phase are formed. The same situation was also found in the case of PAPSAH/PVA blends (*Figures 8* and *9*).

Thermal effect on the structures and electrical conductivities of SPAN/PVA and PAPSAH/PVA blends

The results of the t.g.a. measurements for PVA, SPAN, S5V5, PAPSAH, and P5V5 are shown in *Figure 10*. For the PVA film (curve (*a*)), no appreciable weight loss is observed at temperatures below 200°C. For the SPAN film (curve (*b*)), the weight loss due to the elimination of sulfonic acid groups[43] starts at about 180°C (majority weight loss at 275°C). For the blend S5V5 (curve (*c*)), a two-stage weight loss is exhibited. The first stage starts at about 110°C, which is lower than those of pure PVA and SPAN and results from acid-catalysed dehydration of PVA and a condensation reaction between –OH and a proton (of $-SO_3H$), as revealed below, while the starting temperature for the elimination of sulfonic acid groups remains the same as in SPAN film. For the PAPSAH film, the weight loss starts at about 110°C (majority weight loss at 220°C), while for P5V5 blend (curve (*e*)), the weight loss temperature starts at about 110°C (majority weight loss at 175°C), which is similar to that of PAPSAH (curve (*d*)).

For an understanding of the effects of thermal treatment on the electronic structures of SPAN and PAPSAH in S5V5 and P5V5 blends, solid films of the blends coated on glass plates were heated at 80, 120, and 150°C for 1 h, and then their u.v.–vis spectra at room temperature were recorded as shown in *Figure 11*. As can be observed for both cases, the absorption intensity of the polaron band transition at 880–910 nm decreases and the absorption due to exciton transition of the quinoid rings at about 580–590 nm increases. This implies that a permanent partial thermal undoping occurs, and the conductivity will decrease, as will be described later.

The i.r. spectrum of the blend S5V5 after thermal treatment at 150°C for 1 h (*Figure 5d*) shows that the absorption intensities at 3422 (–OH stretching) and 1147 cm^{-1} (C–O stretching) are reduced and the band at 1173 cm^{-1}, assigned to S=O stretching, shifts to 1176 cm^{-1}, indicating the occurrence of condensation reactions of –OH groups with the protons of $-SO_3H$

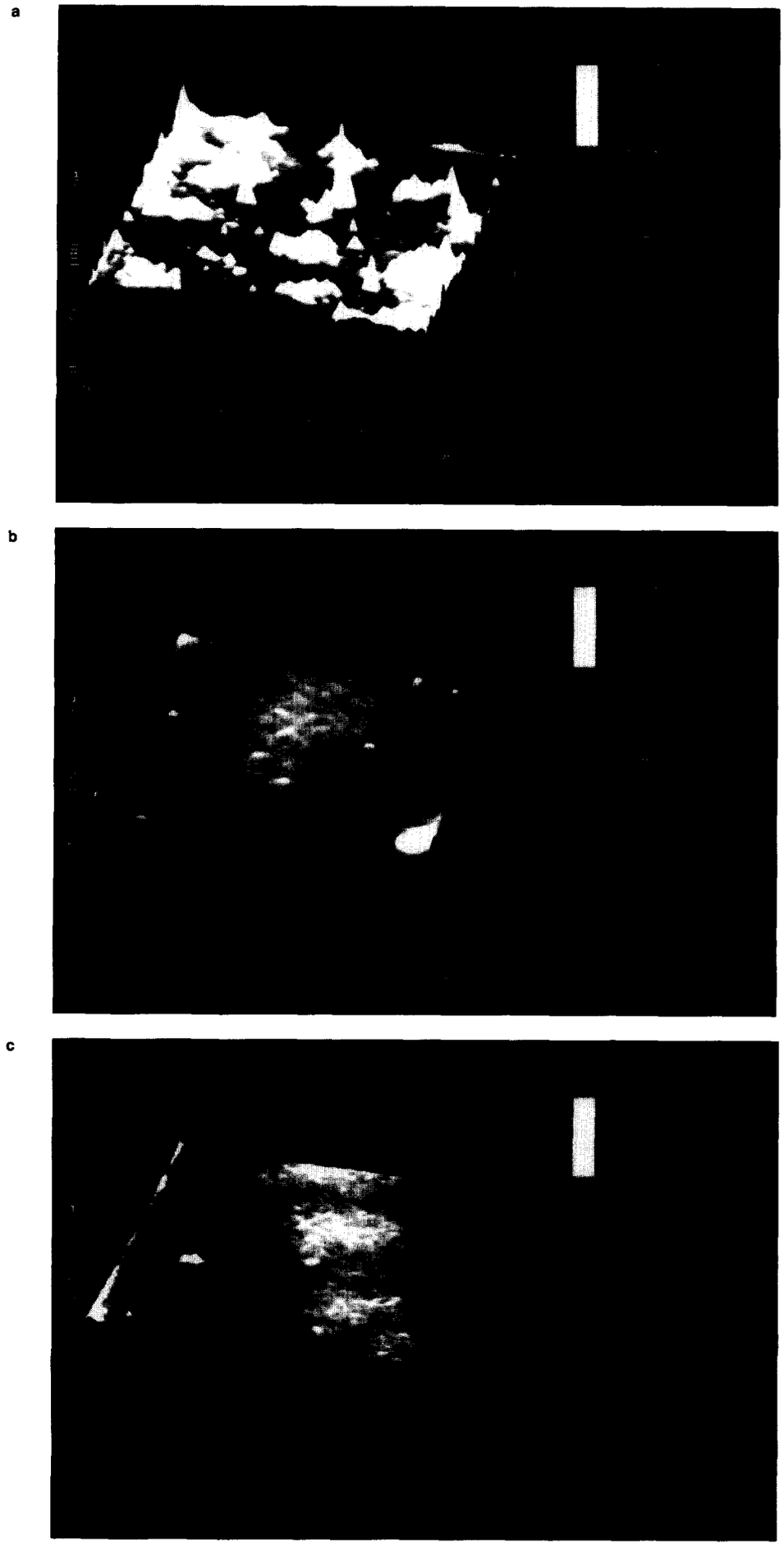

Figure 6 AFM images of (a) SPAN, (b) S9V1, (c) S7V3, (d) S5V5, (e) S3V7, and (f) S1V9 on HOPG substrates

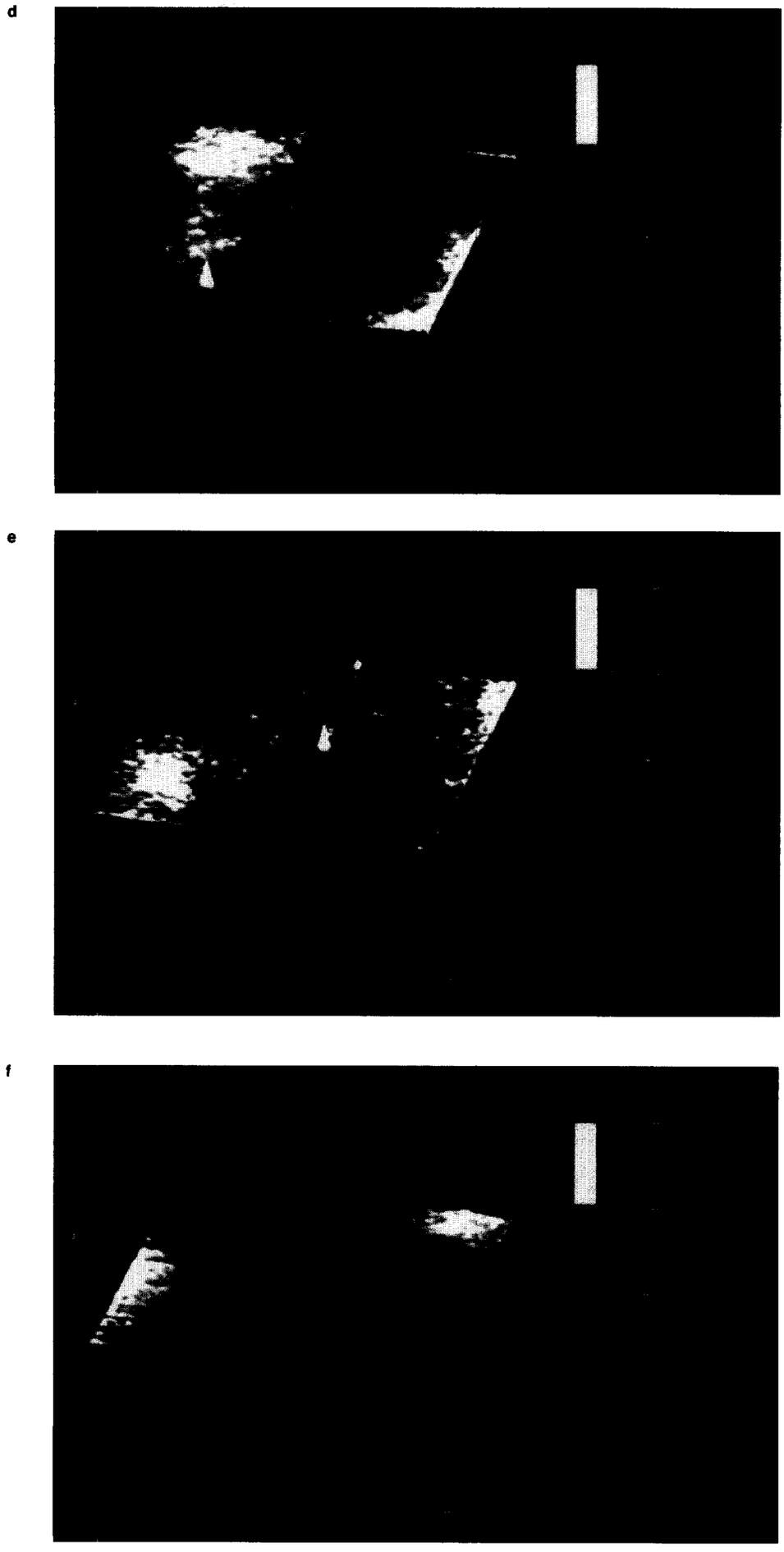

Figure 6 Continued

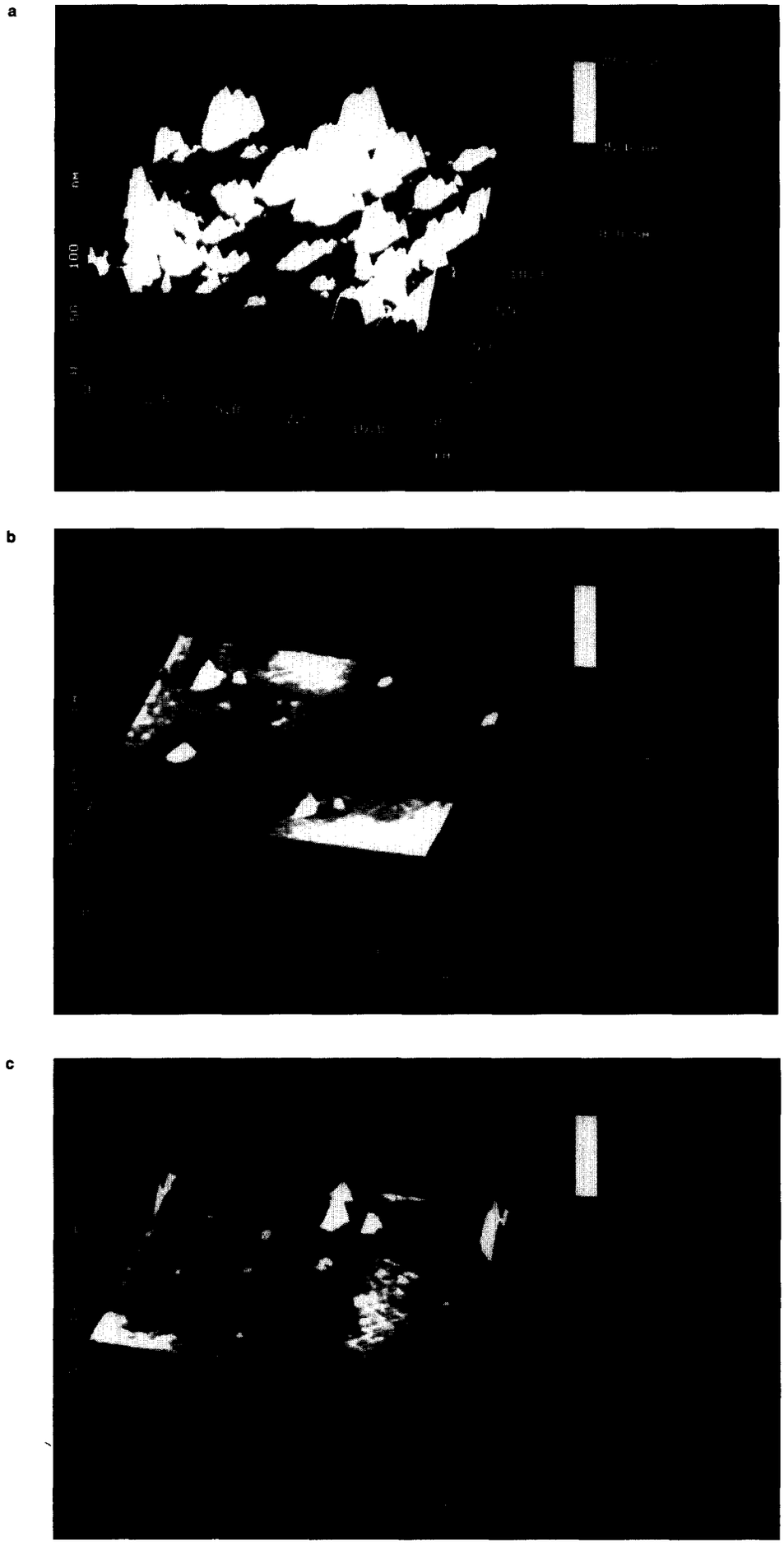

Figure 7 STM images of (a) SPAN, (b) S9V1, (c) S7V3, (d) S5V5, (e) S3V7, and (f) S1V9 on HOPG substrates

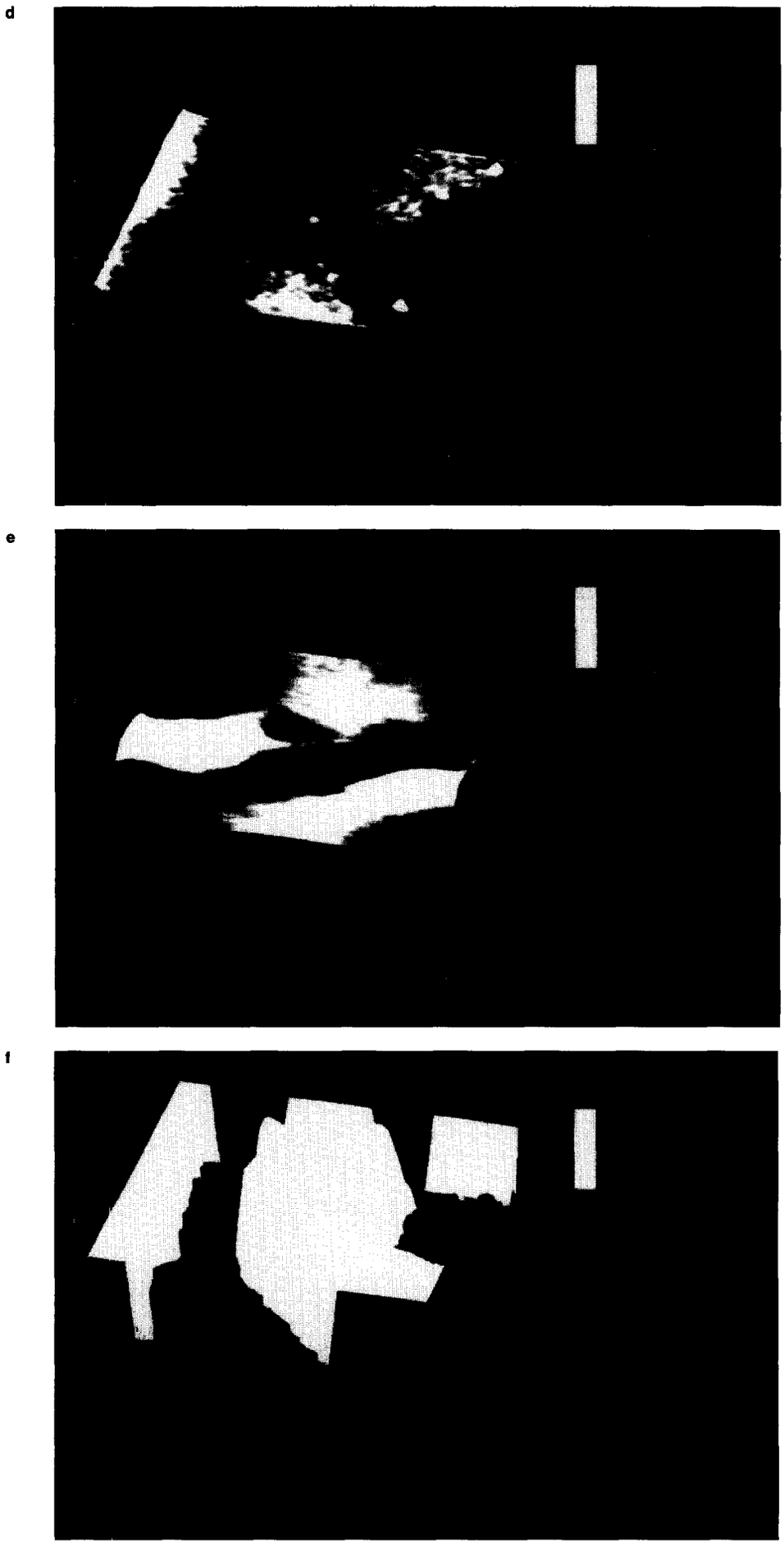

Figure 7 Continued

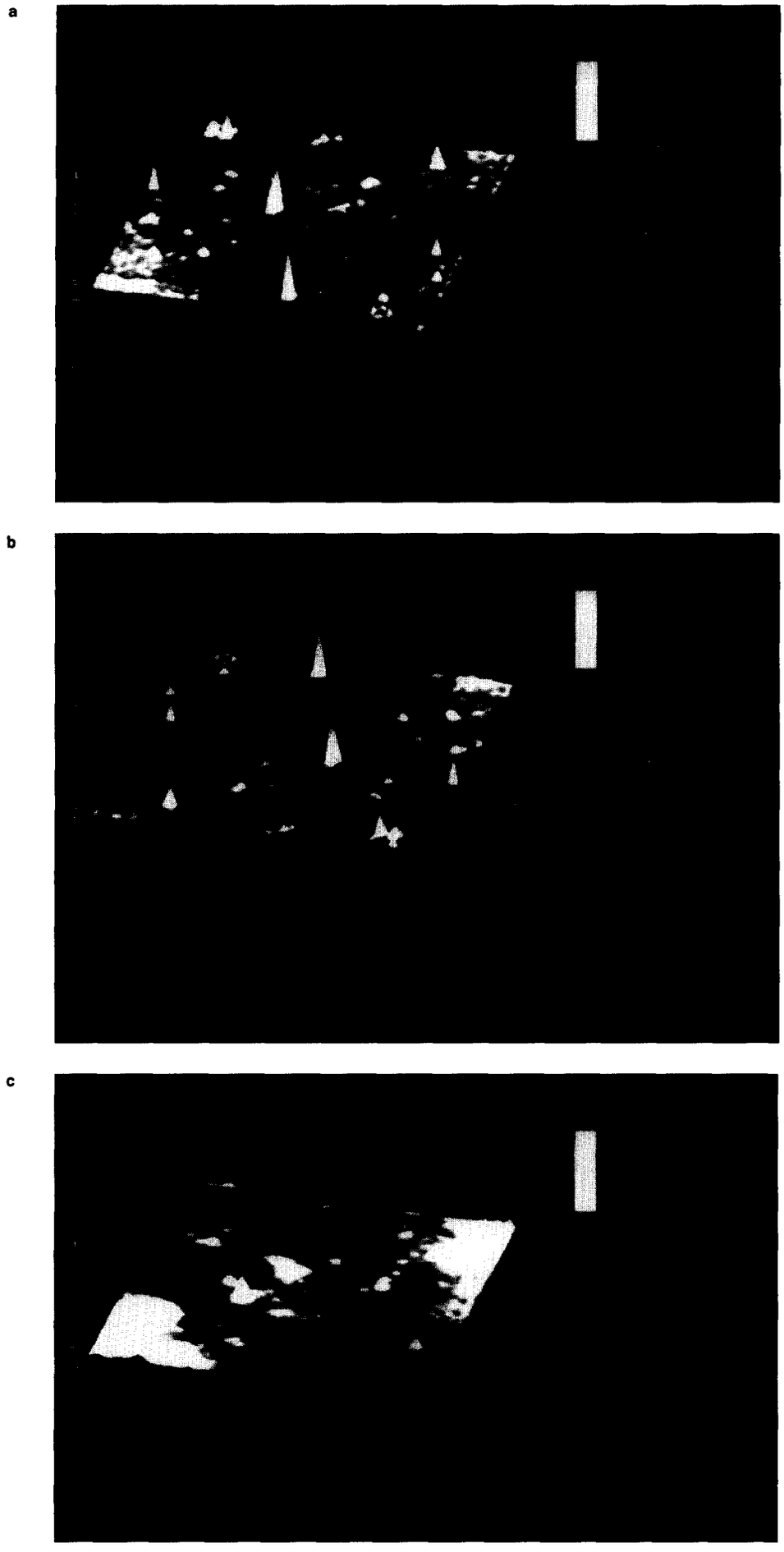

Figure 8 AFM images of (a) P9V1, (b) P5V5, and (c) P1V9 on HOPG substrates

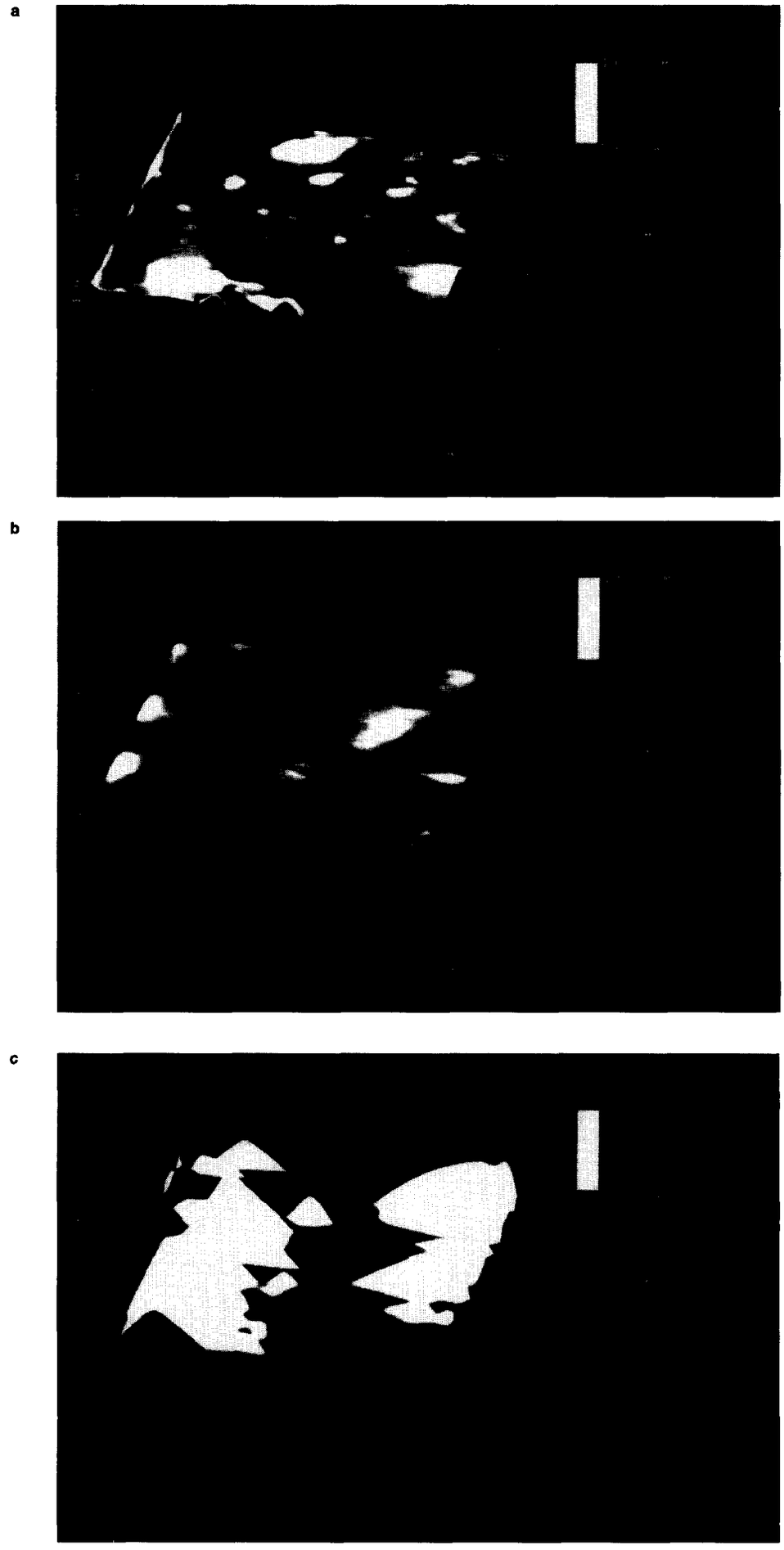

Figure 9 STM images of (a) P9V1, (b) P5V5, and (c) P1V9 on HOPG substrates

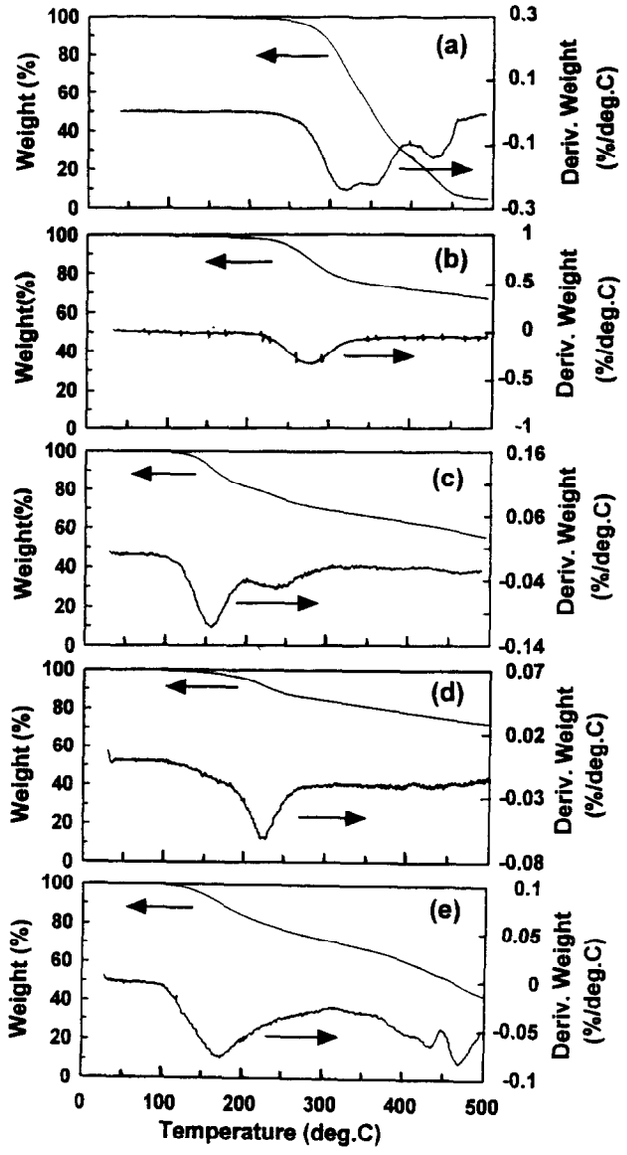

Figure 10 T.g.a. curves of (a) PVA, (b) SPAN, (c) S5V5, (d) PAPSAH, and (e) P5V5

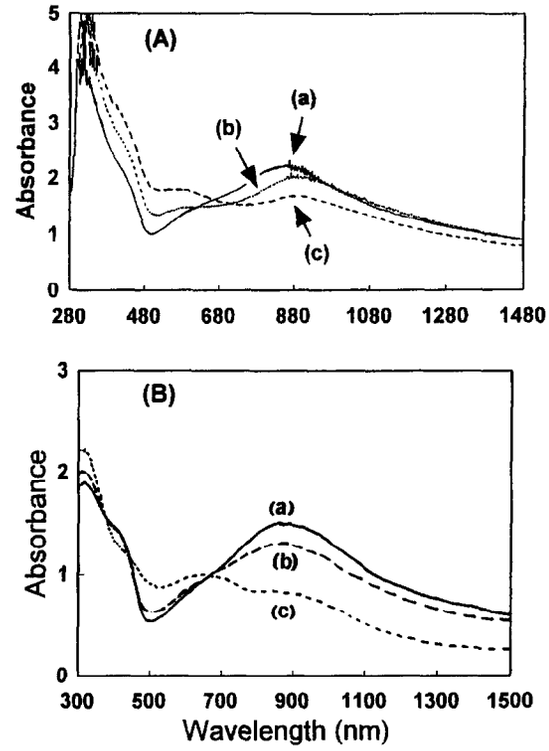

Figure 11 U.v.–vis spectra at room temperature of (A) (a) S5V5 blend film and that after heating at 80°C (indistinguishable) and at (b) 120°C and (c) 150°C; (B) (a) P5V5 blend film and that after heating at 80°C (indistinguishable) and at (b) 120°C and (c) 150°C

groups (which lead to a crosslinked structure) and acid-catalysed dehydration of PVA, as in the case of HBF_4-doped PAn/PVA composite[15]. Also the 1584 (C=C ring stretching of $IP^{+\cdot}$) and 1482 cm^{-1} (C=C stretching of benzenoid ring[49]) bands shift to 1590 and 1504 cm^{-1}, respectively, and the absorption intensity ratio of the former to the latter is reduced after the heating, indicating the occurrence of the crosslinking reaction through a conversion of quinoid rings to benzoid rings[52]. For the blend of PAPSAH and P5V5, similar results were observed. After thermal treatment at 150°C for 1 h, its i.r. spectrum (*Figure 5f*) shows that the absorption intensities at 3410 cm^{-1} (–OH stretching) and 1155 cm^{-1} (C–O stretching) are reduced and the band at 1173 cm^{-1} (S=O stretching) shifts to 1180 cm^{-1}. The 1581 and 1492 cm^{-1} bands shift to 1586 and 1498 cm^{-1}, respectively, and the absorption intensity ratio of the former to the latter is reduced after the heating. Therefore the S5V5 and P5V5 blends were thermally undoped, accompanying a loss of majority of the polarons after the thermal treatment, which is consistent with the results of the u.v.–vis measurements above, and the concomitant loss of conductivity as discussed later.

The temperature dependence of the conductivities of the SPAN/PVA blends, S5V5 and S3V7, was measured as shown in *Figure 12*, and the characteristic results are listed in Table 1, including conductivity at room

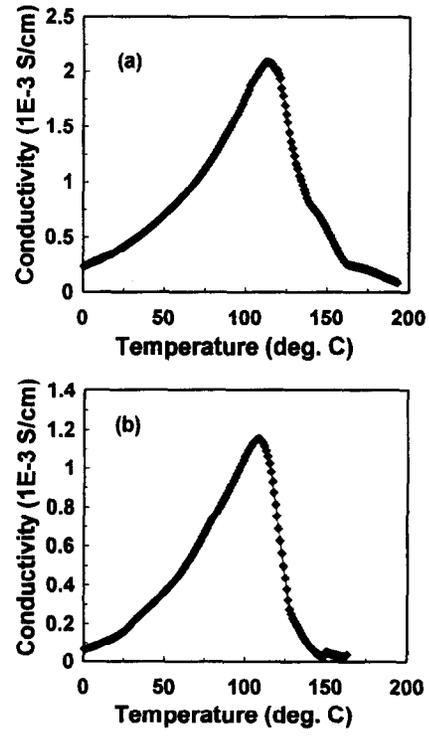

Figure 12 Conductivity vs temperature of (a) S5V5 and (b) S3V7

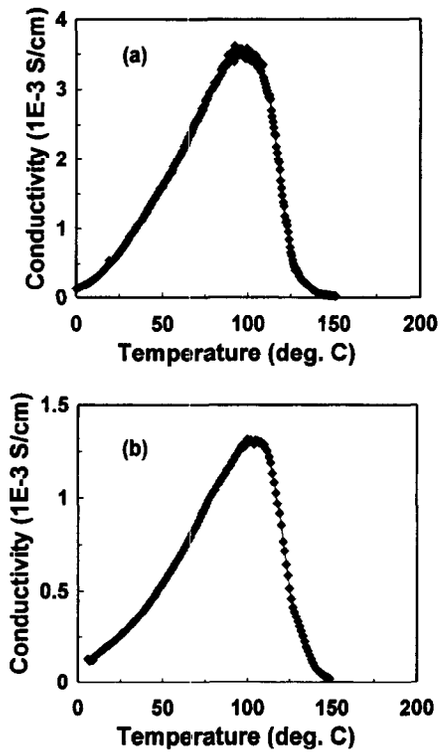

Figure 13 Conductivity vs temperature of (a) P5V5 and (b) P3V7

temperature, the temperature at which the conductivity reaches a maximum, and maximum conductivity. For S5V5 blend (*Figure 12a*), the conductivity increases with temperature from 0 to 115°C (the maximum $2.2 \times 10^{-3}\,S\,cm^{-1}$) and decreases from 115 to 190°C. That conductivity drops above 115°C can be attributed to the occurrence of thermal undoping, as revealed in the u.v.–vis, i.r., and t.g.a. sections above. Similar results were also observed for S3V7 blend (*Figure 12b*), while the conductivity reaches a maximum ($1.2 \times 10^{-3}\,S\,cm^{-1}$) at 110°C. As can be seen, the thermal undoping temperature of the SPAN/PVA blends are much lower than that of SPAN (190°C)[43]. This can be attributed to the occurrence of dehydration of the PVA catalysed by the sulfonic acid group in SPAN and the condensation reaction between the –OH group and proton as revealed in the t.g.a. and i.r. section above. For the PAPSAH/PVA blends, the temperature dependence of the conductivity was measured as shown in *Figure 13*, and the characteristic results are listed in *Table 2*. As shown in *Figure 13*, the conductivities of P5V5 and P3V7 increase with temperature from 0 to 100–110°C (the maxima, 4×10^{-3} and $1 \times 10^{-3}\,S\,cm^{-1}$ respectively) and then decrease until 150°C. The occurrence of conductivity maxima at 100–110°C is nearly the same as that of PAPSAH. Thus the drop of conductivity above 100–110°C of P5V5 and P3V7 blends can be attributed to the occurrence of thermal undoping with a loss of the polarons of the PAPSAH in the blends, as revealed in the u.v.–vis, i.r. and t.g.a. sections above.

CONCLUSION

The incorporation of the water soluble polymer PVA into the water soluble self-acid-doped conducting PAns, SPAN and PAPSAH, has no effect on their doping levels. This can be attributed to the higher basicity of the –N= unit than –OH, causing a more favourable interaction of the $-SO_3H$ group with –N=. The strong interaction of these PAns with PVA through hydrogen bonding between hydroxyl groups (of PVA) and amine and positively charged amine and imine sites (of SPAN and PAPSAH) leads to a partial miscibility. As the PVA content is minor (lower than 50 wt%) it disperses in the SPAN matrix fairly well. As PVA is the major component (higher than 70 wt%), interconnected regions of PVA-rich phase and of SPAN-rich phase are formed, such that the dilution effect of PVA on the conductivity is not large. Although SPAN has a higher thermal undoping temperature at 190°C, it drops to 110°C after blending with PVA due to the occurrence of dehydration at this temperature. For PAPSAH, its thermal undoping temperature (110°C) remains nearly unchanged after blending with PVA.

ACKNOWLEDGEMENT

We wish to thank the National Science Council of R.O.C. for financial aid through project NSC 84-2221-E007-023.

REFERENCES

1. MacDiarmid, A. G., Chiang, J. C., Halpern, M., Huang, W. S., Mu, S. L., Somasiri, N. L. D., Wu, W. and Yaniger, S. I., *Mol. Cryst. Liq. Cryst.*, 1985, **121,** 173.
2. Chiang, J. C. and MacDiarmid, A. G., *Synth. Met.*, 1986, **13,** 193.
3. MacDiarmid, A. G., Chiang, J. C., Richter, A. F. and Epstein, A. J., *Synth. Met.*, 1987, **18,** 285.
4. Naarman, H., *Adv. Mater.*, 1990, **2,** 345.
5. Genies, E. M., Hany, P. and Santier, C. J., *J. Appl. Electrochem.*, 1988, **18,** 285.
6. Kaneko, M. and Nakamura, H., *J. Chem. Soc., Chem. Commun.*, 1985, 346.
7. Paul, E. W., Rico, A. J. and Wrighton, M. S., *J. Phys. Chem.*, 1985, **89,** 1441.
8. Huang, W. S., Lecorre, M. A. and Tissier, M., *J. Vac. Sci. Technol.*, 1991, **B9,** 3428.
9. Chen, S. -A. and Fang, Y., *Synth. Met.*, 1993, **60,** 215.
10. Kitani, A., Yano, J. and Sasaki, K., *J. Electroanalyt. Chem.*, 1986, **209,** 227.
11. Jelle, B. P. and Hagen, G., *J. Electrochem. Soc.*, 1993, **140,** 3560.
12. Wood, A. S., *Modern Plastic Int.*, 1991, Aug., 3.
13. Epstein, A. J. and Yue, J. US Patent No. 5137991, 1992.
14. Huang, W. S., Humphrey, B. D. and MacDiarmid, A. G., *J. Chem. Soc., Faraday Trans. 1*, 1986, **82,** 2385.
15. Chen, S.-A. and Fang, W.-G., *Macromolecules*, 1991, **24,** 1242.
16. Leclerc, M., Guay, J. and Dao, L. H., *Macromolecules*, 1989, **22,** 649.
17. Wei, Y., Focke, W. W., Wnek, G. E., Ray, A and MacDiarmid, A. G., *J. Phys. Chem.*, 1989, **93,** 495.
18. Macinnes, D. and Fint, B. C., *Synth. Met.*, 1988, **25,** 235.
19. Ito, A., Ota, K.-I., Tanaka, K., Yamabe, T. and Yoshizawa, K., *Macromolecules*, 1995, **28,** 5618.
20. Watanabe, A., Mori, K., Iwabuchi, Y., Iwasaki, Y., Nakamura, Y. and Ito, O., *Macromolecules*, 1989, **22,** 5321.
21. Chevalier, J. W., Bergeron, J.-Y. and Dao, L. H., *Macromolecules*, 1992, **25,** 3325.
22. Manohar, S. K., MacDiarmid, A. G., Cromack, K. R., Ginder, J. M. and Epstein, A. J., *Synth. Met.*, 1989, **29,** E349.
23. Chan, H. S. O., Ho, P. K. H., Ng, S. C., Tan, B. T. G. and Tan, K. L., *J. Am. Chem. Soc.*, 1995, **117,** 8517.
24. Wei, Y., Harihara, R. and Patel, S. A., *Macromolecules*, 1990, **23,** 758.
25. Bergeron, J. Y. and Dao, L. H., *Macromolecules*, 1992, **25,** 3332.
26. Pandey, S. S., Annapoorni, S. and Malhotra, B. D., *Macromolecules*, 1993, **26,** 3190.
27. Nguyen, M. T., Kasai, P., Miller, J. L. and Diaz, A. F., *Macromolecules*, 1994, **27,** 3625.

28. Nguyen, M. T. and Diaz, A. F., *Macromolecules*, 1994, **27,** 7003.
29. Nguyen, M. T. and Diaz, A. F., *Macromolecules*, 1995, **28,** 3411.
30. Yue, J. and Epstein, A. J., *J. Am. Chem. Soc.*, 1990, **112,** 2800.
31. Yue, J., Wang, Z. H., Cromack, K. R., Epstein, A. J. and MacDiarmid, A. G., *J. Am. Chem. Soc.*, 1991, **113,** 2665.
32. Bergeron, J. Y., Chevalier, J. W. and Dao, L. H., *J. Chem. Soc., Chem. Commun.*, 1990, 180.
33. Chen, S.-A. and Hwang, G.-W., *J. Am. Chem. Soc.*, 1994, **116,** 7939.
34. Chen, S.-A. and Hwang, G.-W., *J. Am. Chem. Soc.*, 1995, **117,** 10055.
35. Zheng, W.-Z., Levon, K., Laakso, J., and Osterholm, J.-E., *Macromolecules*, 1994, **27,** 7754.
36. Cao, Y., Smith, P. and Heeger, A. J., *Synth. Met.*, 1992, **48,** 91.
37. Cameron, R. E. and Clement, S. K., US Patent 5008041, 1991.
38. Chan, H. S. O., Gau, L. M., Chew, C. H., Ma, L. and Seow, S. H., *J. Mater. Chem.*, 1993, **3,** 1109.
39. Liu, J. -M. and Yang, S. C., *J. Chem. Soc., Chem. Commun.*, 1991, 1259.
40. Angelpoulos, M., Patel, N., Shaw, J. M., Lanianca, N. C. and Rishton, S. A., *J. Vac. Sci. Technol. B*, 1993, **11,** 2794.
41. Shannon, K. and Fernandez, J. E., *J. Chem. Soc., Chem. Commun.*, 1994, 643.
42. Liao, Y. J. and Levon K., *Macromol Rapid Commun.*, 1995, **16,** 643.
43. Chen, S.-A. and Hwang, G.-W., *Macromolecules*, 1996, **29,** 3950.
44. Bunn, C. W., *Nature*, 1948, **161,** 929.
45. Lu, F. L., Wudl, F., Nowak, M. and Heeger, A. J., *J. Am. Chem. Soc.*, 1986, **108,** 8311.
46. Stafstrom, S., Breadas, J. L., Epstein, A. J., Woo, H.-S., Tanner, D. B., Huang, W.-S. and MacDiarmid, A. G., *Phys. Rev. Letters*, 1987, **59,** 1464.
47. Epstein, A. J., Ginder, J. M., Zuo, F., Bigelow, R. W., Woo, H.-S., Tanner, D. B., Richter, A. F., Huang, W.-S. and MacDiarmid, A. G., *Synth. Met.*, 1987, **16,** 303.
48. Furukawa, Y., Ueda, F., Hyodo, Y., Harada, I., Nakajima, T. and Kawagoe, T., *Macromolecules*, 1988, **21,** 1297.
49. Harada, I., Furukawa, Y. and Ueda, F., *Synth. Met.*, 1989, **29,** E303.
50. Tadokoro, H., Seki, S. and Nitta, I., *Bull. Chem. Soc. Jpn.*, 1995, **28,** 559.
51. Yang, C. Y., Cao, Y., Smith, P. and Heeger, A. J., *Synth. Met.*, 1993, **53,** 293.
52. Chen, S.-A. and Lee, H.-T., *Macromolecules*, 1993, **26,** 3254.